energies

MDPI

Article

Improving Fuel Economy and Engine Performance through Gasoline Fuel Octane Rating

José Rodríguez-Fernández [1,*], Ángel Ramos [1], Javier Barba [1], Dolores Cárdenas [2] and Jesús Delgado [2]

[1] Escuela Técnica Superior de Ingeniería Industrial, University of Castilla—La Mancha, 13071 Ciudad Real, Castilla–La Mancha, Spain; angel.ramos@uclm.es (Á.R.); Javier.Barba@uclm.es (J.B.)
[2] Repsol Technology Lab, 28935 Móstoles, Madrid, Spain; mdcardenasa@repsol.com (D.C.); jdelgadod@repsol.com (J.D.)
* Correspondence: jose.rfernandez@uclm.es

Received: 19 June 2020; Accepted: 2 July 2020; Published: 7 July 2020

Abstract: The octane number is a measure of the resistance of gasoline fuels to auto-ignition. Therefore, high octane numbers reduce the engine knocking risk, leading to higher compression threshold and, consequently, higher engine efficiencies. This allows higher compression ratios to be considered during the engine design stage. Current spark-ignited (SI) engines use knock sensors to protect the engine from knocking, usually adapting the operation parameters (boost pressure, spark timing, lambda). Moreover, some engines can move the settings towards optimized parameters if knock is not detected, leading to higher performance and fuel economy. In this work, three gasolines with different octane ratings (95, 98 and 100 RON (research octane number)) were fueled in a high-performance vehicle. Tests were performed in a chassis dyno at controlled ambient conditions, including a driving sequence composed of full-load accelerations and two steady-state modes. Vehicle power significantly increased with the octane rating of the fuel, thus decreasing the time needed for acceleration. Moreover, the specific fuel consumption decreased as the octane rating increased, proving that the fuel can take an active part in reducing greenhouse gas emissions. The boost pressure, which increased with the octane number, was identified as the main factor, whereas the ignition advance was the second relevant factor.

Keywords: octane number; knocking; spark-ignition; performance; knock sensor; fuel economy; vehicle acceleration

1. Introduction

The European Union (EU) has recently committed to achieving carbon neutrality by 2050 [1]. This goal necessarily involves diminishing CO_2 emissions in the transport sector, responsible for 27% of total European greenhouse gas (GHG) emissions [2]. In this sector, well-to-wheel (WtW) analyses estimate the GHG emissions associated with the fuel, inventorying emissions in feedstock-related (or primary fuel-related) stages, fuel-related stages and final fuel use in the vehicle. The last step is known as tank-to-wheel emissions, which can be mitigated through fuel formulation and more efficient vehicle and engine technologies. For this reason, present and future research on engines pursues increasing the efficiency [3,4], thus achieving better fuel economy and lower CO_2 emissions.

In the case of spark-ignited (SI) engines, direct injection (DI) and, more recently, downsizing, turbocharging and high compression ratios are the main working areas for increasing their efficiency. However, all these approaches are constrained by the appearance of abnormal combustion regimes. The fuel itself is fundamental for overcoming this limitation, and fuel manufacturers can accompany GHG reduction by developing high-octane gasolines that could be properly exploited by current SI

engine technologies. This way, fuel and engine technologies interact synergistically, with the fuel enabling the engine to work on more efficient conditions. CONCAWE (Environmental Science for European Refining, an association of companies that operate petroleum refineries in the EU) [5] recently modelled and tested the potential of high-octane gasolines to enhance the efficiency of downsized, high-compression ratio SI engines (whose share in the market is expected to grow according to the current trends). The highest-octane fuel (102 RON—Research Octane Number) improved fuel economy around 4% in driving cycles, compared to 95 RON.

The anti-knocking tendency of a gasoline has been traditionally described by the octane numbers, the research octane number (RON) and the motor octane number (MON, measured under more stressed testing conditions), both included in EN 228 Standard for unleaded petrol quality. However, some studies show that in current SI engines MON is no longer a good indicator and higher MON can indeed be unfavourable to engine performance [6]. In the EU, gasoline vehicles must operate safely with regular 95 RON fuel, but there is a range of vehicles that can take advantage of higher-octane gasolines to increase the efficiency when running under adverse conditions (high ambient temperature, full-load accelerations) [5].

The most common undesired combustion phenomenon is knock [7] (although cases of benign knock that leads to higher efficiency have been reported [8]), but other unwanted regimes are super-knock and pre-ignition [7]. Knock, or knocking, occurs when the fuel-air mixture in the unburnt gas zone auto ignites ahead of the flame front. The presence of hot spots and higher temperature and pressure (the above-referred trends in SI engines contribute to these) in the combustion chamber makes knock more probable, as well as low speed and high load conditions. With the strengthening of turbocharging and downsizing, super-knock (a knock phenomenon at higher intensity than usual) has been documented and explained based on developing detonations [9]. Pre-ignition is caused by hot spots inside the combustion chamber, such as deposits in the spark plugs and valves [10]. However, in modern DI engines the most probable cause for pre-ignition is the accumulation of lubricant droplets in the chamber when the fuel spray impinges the cylinder walls [11]. This and other causes have been reviewed in [12]. Pre-ignition typically occurs in the compression stroke, earlier than the command from the spark plug, and thus decreases the efficiency and the power. Pre-ignition makes more likely the appearance of super-knock [13].

A few transient episodes of abnormal combustion are not dangerous [3]. However, prolonged operation deteriorates the engine performance, damages the engine (pistons and electrodes, mainly) [14], thus affecting engine reliability and durability, and produces noise and driver annoyance. Hence, detecting and suppressing knock is essential.

Although there are other methods (based on noise measurements [15]), knock can be mainly detected with a pressure sensor located inside the cylinder (or several cylinders) or using a vibration sensor (called "knock" sensor). The first is typical in research and development applications, sometimes in combination with optical techniques [16], as this provides a complete understanding of the combustion. When the amplitude of the pressure fluctuations exceeds a threshold, the engine is knocking [4]. By contrast, most commercial vehicles are equipped with knock sensors, which are accelerometers that sense the vibrations that knocking and uneven combustion in the cylinders cause in the engine block. The output signal of the sensor is informed to the engine control unit (ECU) to decide a corrective action that returns the engine to regular combustion, despite this implying a power reduction or/and fuel economy penalization.

The most acknowledged corrective action consists in retarding the ignition [17,18]. Other measures include changing the intake valve timing to reduce the effective compression ratio [19], enriching the fuel–air mixture [20] (for the excess fuel to act as a charge cooler), using EGR [21], specially cooled EGR [22] (because EGR prolongs the ignition delay time of the unburnt gas, cooling the intake charge [23]) or limiting the boost pressure [24], among others. Today, knock sensors are essential not only for ensuring durability but also for improving the engine efficiency and fuel economy and for reducing emissions.

In current SI engines, for a given operating point and fuel, advancing the spark timing increases the engine efficiency but also the knock probability [4]. The spark advance for which the knock intensity is unacceptable is called knock-limited spark advance (KLSA) [25], and this is usually achieved earlier than the spark advance for maximum efficiency (maximum brake torque, MBT). The latest trends in SI engines (turbocharging, higher compression ratios) have indeed accentuated this difference, thus enlarging the potential of high-octane gasolines to increase the efficiency.

Some works evaluate the effects of high-octane gasolines in SI engines. In [26], the authors noticed that a higher octane gasoline increased torque and power only in an engine with a knock control system. Stradling et al. [6] tested acceleration sequences with different octane rating gasolines (including ethers and alcohols) in two passenger cars equipped with knock sensors. The acceleration time decreased (power increased) and the energy consumption deteriorated with the octane number, this trend being more accentuated in the low-octane range. Moreover, both variables fitted better with RON than MON (higher MON was detrimental, actually). Although the effect of the octane number on the emissions was also explored, emissions are affected by the fuel molecular structure as well. Shuai et al. [27] tested five vehicles and found different sensitivities to the fuel. The effect of the octane number was more notable at high speed and load. On average, they reported 1% better fuel economy per unit of RON.

In the present work, three gasoline fuels meeting all requirements of EN 228 Standard, with regular (95 RON), middle (98 RON) and high octane (100 RON), have been tested in a passenger car at full load conditions in both accelerations and steady-state modes; 100 RON gasoline was prepared with a N-aquil substituted aniline as octane booster, which has not been tested in high-performance commercial vehicles yet. The results include not only fuel consumption, thermal efficiency and CO_2 emissions, but also the rest of the gaseous-regulated emissions (CO, total hydrocarbon (THC), NOx) for a complete evaluation of the fuels. The study aligns with the trend in the fuel market towards high-octane gasolines to support the introduction and consolidation of higher efficiency engines. In fact, the recent update of the Worldwide Fuel Charter [28] released by the main automobile associations introduces a new gasoline category, characterized by high octane numbers mainly, intended for the most stringent markets in terms of CO_2 targets.

2. Materials and Methods

2.1. Experimental Setup

The study was carried out on a two-wheel drive (2WD) chassis dynamometer Schenk for light-duty vehicles, which is located inside a climatic chamber (Figure 1). It is equipped with a single roller (159.5 cm diameter, 168 kW nominal power) which simulates the rolling and the aerodynamic resistances, as well as the equivalent vehicle inertia. The pressure and temperature sensors required are located according to [29]. The blower (placed in front of the vehicle) is used to produce cooling wind at the simulated vehicle velocity. Inside the climatic chamber, the ambient temperature can be regulated from −20 °C to 40 °C.

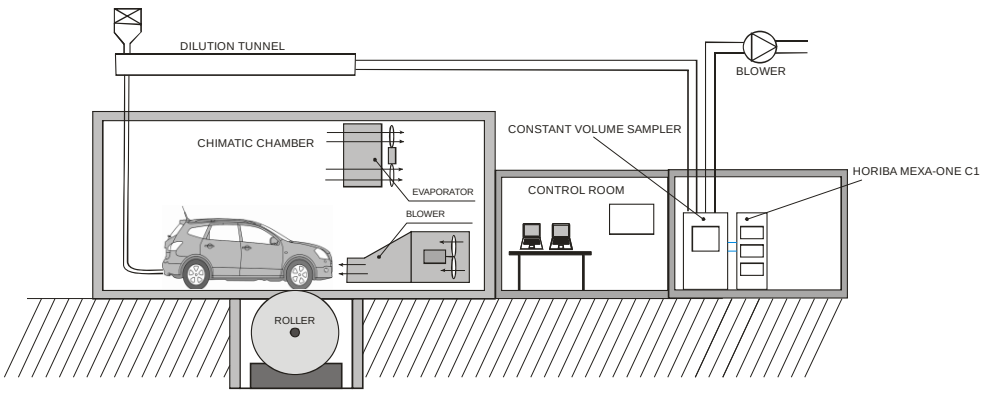

Figure 1. Scheme of the experimental setup.

The total exhaust gas flow rate emitted by the vehicle is diluted with filtered atmospheric air in a total dilution tunnel Horiba DLT-7040. The pollutant emissions were measured both continuously (time-resolved) and after a small diluted gas sample was collected in bags. Gaseous emissions were measured with a Horiba MEXA-ONE C1 analyser. It is equipped with separate modules for the measurement of nitrogen oxides, carbon dioxide, carbon monoxide and total hydrocarbons. Sampling probes and transport lines from the measurement point (dilution tunnel) were heated at 191 °C to avoid condensation of hydrocarbons. The specifications of the equipment are shown in Table 1. All measurements were previously synchronised, since the response time of each module and the delay time in the transport lines are different.

Table 1. Specifications of Horiba MEXA-ONE C1.

Carbon Monoxide Module	
Measurement method	Non-dispersive infrared (NDIR)
Range	0–5000 ppm
Accuracy	3% (of measured value)
Carbon Dioxide Module	
Measurement method	Non-dispersive infrared (NDIR)
Range	0–1000 ppm
Accuracy	3.1% (of measured value)
Nitrogen Oxides Module	
Measurement method	Chemiluminescence (CLD), vacuum
Range	0–5000 ppm
Accuracy	2.7% (of measured value)
Total hydrocarbon module	
Measurement method	Flame ionization detector (FID)
Range	0–60,000 ppm
Accuracy	2.7% (of measured value)

Regarding fuel consumption, this was calculated based on the carbon balance (CO_2, CO and THC) with the method proposed by Directive 1151/2017 of the European Commission [29]. An Opel Corsa OPC equipped with a spark-ignition indirect injection (SI-IDI) engine was selected for the tests (Table 2). This is a commercial high-performance vehicle with maximum power within the limits of the experimental facility. The vehicle was not modified prior to gasoline testing in order to identify real advantages on vehicles available in the current market, without considering future design improvements that are expected and have been discussed in other works. The engine control strategy of the vehicle was not modified from the original one; therefore, the results are expected to reproduce well the on-road performance and emissions. Several variables were measured and recorded through OBD (on-board diagnostics), such as vehicle velocity, accelerator pedal position, boost pressure, lambda sensor or spark timing, among others, in order to evaluate the vehicle performance and support the trends observed.

2.2. Fuels

The samples used in this study present different antiknock properties and satisfy the specifications for winter gasoline EN-228 for a maximum quantity of oxygen of 2.7% (E5). Two of them are commercial type, sampled from Company Service Stations, representing the grades distributed in Spain (95 RON and 98 RON). The third gasoline is a modification of 98 RON commercial gasoline by using an octane booster, with a target of 100 RON. Octane booster is an N-aquil substituted aniline with high efficiency to increase RON without relevant changes in the rest of the properties.

Table 2. Specifications of Opel Corsa OPC.

Emission Regulation	Euro 6b
Engine type	SI-IDI, turbocharged, intercooler
Compression ratio	8.8:1
Power @ 5800 rpm	152 kW
Torque @ 1.900–5.800 rpm	280 Nm
Displacement	1.598 cm^3
Bore	79 mm
Stroke	81.5 mm
Gearbox	Manual
Valves per cylinder	4
Octane number (RON) recommended [1]	100
Total gear ratio (km/h each 1000 rpm)	
1st	7.2
2nd	12.7
3rd	20.3
4th	28.6
5th	35.7
6th	44.6

[1] As specified by the vehicle manufacturer.

Table 3 shows the key properties of the different evaluated samples. The heating values of all fuels were similar. The small differences were within the reproducibility of the testing (ASTM D240). The selection of the samples answered to the need to identify the advantages of using high-octane gasolines, compared to standard gasoline. Performance, consumption and emissions will define the added value to the customer and the potential of each product. The 100 RON gasoline is a new high-octane product in Spanish market. Therefore, a rigorous measurement of improvements with respect to existing products was the key objective of this study.

Table 3. Properties of tested gasolines.

Test	Method	Units	95 RON	98 RON	100 RON
Research Octane Number	ASTM* D 2699-18a	–	96.1	98.1	99.7
Motor Octane Number	ASTM D 2700-18a	–	85.1	87.4	87.8
Density 15 °C	ASTM D 4052-18	kg/m^3	733	735	737
Vapor pressure (DVPE)	ASTM D 5191-15	kPa	67.1	72.5	71.9
Vapor Lock Index	EN 228	–	903	949	951
Sulphur	ASTM D 4294-16e1	mg/kg	9	10	10
Lead	EN 237:2005	mg/L	<5.0	<5.0	<5.0
Existent Gums	ASTM D 381-12 (2017)	mg/100 mL	<0.1	<0.1	<0.1
Distillation					
Evaporated 70 °C (E70)	ASTM D 86-17	% *v/v*	33.1	32.0	33.2
Evaporated 100 °C (E100)		% *v/v*	56.3	55.9	57.2
Evaporated 150 °C (E150)		% *v/v*	82.7	82.6	83.8
Final Boiling Point		°C	194.8	191	198.0
Residue		% *v/v*	1.0	1.1	1.0
Hydrocarbons					
Olefins	EN ISO 22854:2016	% *v/v*	13.0	11.1	11.1
Aromatics		% *v/v*	27.9	24.4	24.4
Benzene		% *v/v*	0.5	0.7	0.7
Oxygen		% m/m		2.4	2.4
Methanol		% *v/v*	<0.1	<0.1	<0.1
Ethanol		% *v/v*	1.2	0.7	0.7
Isopropyl alcohol		% *v/v*	<0.5	<0.5	<0.5
ETBE		% *v/v*	7.48	13.5	13.5
Other oxygenated compounds		% *v/v*	<0.1	<0.1	<0.1

* American Society for Testing and Materials.

2.3. Test Protocol

Firstly, the aerodynamic and rolling resistance of the vehicle (road load coefficients) were calculated in order to be replicated in the chassis dyno. The determination of the road load coefficients was performed following the methodology proposed by Regulation 1151/2017 of the European Commission, sub-annex 4, paragraph 4 [29]. Tests were carried out on a straight and flat local road (CM-4117, Spain). The methodology consists in warming up the vehicle and subsequently accelerating up to 140 km/h; after that, coastdown is started with the gearbox in neutral until 20 km/h. Four repeats were performed in opposite directions and wind conditions and ambient temperature were measured. The coastdown time measurements were used to calculate the road load coefficients according to the mentioned regulation.

Coastdown coefficients were subsequently adapted to the chassis dyno in order to replicate real conditions on the road through the roller. For this task, the methodology followed the one proposed by Regulation 1151/2017 of the European commission, sub-annex 4, paragraph 7 and 8 [29].

All tests were carried out at 35 °C (ambient temperature set in the chassis dyno) and the total flow used in the dilution tunnel was 14 m^3/min. The cycle designed for these tests (Figure 2) comprises 10 full-load accelerations from 30 km/h to 162 km/h (toothsaw-type [6], all carried out in fourth gear), followed by two steady-state working points. Prior to the 10 toothsaw, a 10-min warming up at 80 km/h was carried out. Before each toothsaw acceleration, a 2-min period at 30 km/h is driven to ensure that all engine parameters are stable before starting the accelerations. Once the vehicle reaches 162 km/h, it remains at this velocity for 5 s, approximately. Finally, the vehicle slows down at constant deceleration to reach 30 km/h again.

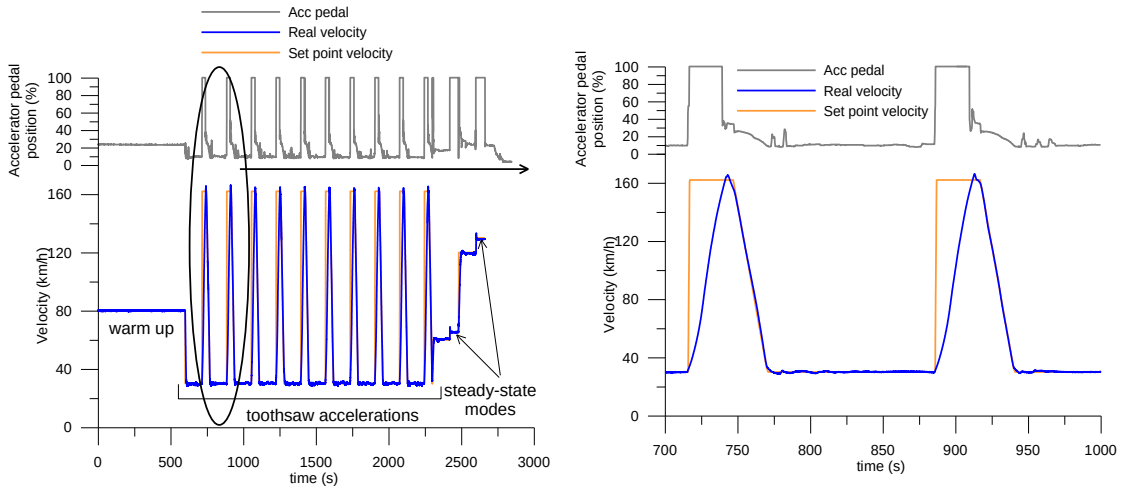

Figure 2. Driving cycle (**left**) and detail of the first accelerations (**right**).

The two steady-state operation modes were selected at 65 km/h and 129 km/h in fourth gear and full-load conditions (around 2500 rpm and 5000 rpm, respectively). The engine was maintained for one minute at each working mode and the results shown in this work are the average for this time period (after discarding the first 15 s, where the variables were not steady yet). Each mode was preceded by an intermediate mode at low load to ensure the vehicle is properly cooled down before carrying out the full-load modes. The whole cycle (setpoint and real velocity-time traces, along with the accelerator position) is shown in Figure 2 left. Moreover, in order to observe clearly the differences between targeted and real speed, Figure 2 right enlarges a small part of the cycle showing the first two toothsaw accelerations.

For the fuel changes, the fuel tank and fuel lines were drained and refilled with the new fuel. After this, a driving cycle (WLTC) was carried out to ensure a complete purge of the fuel supply system.

3. Results and Discussion

The most important performance parameters, such as acceleration, power output and fuel consumption, are firstly analysed for the three fuels at both engine conditions (toothsaw accelerations and steady-state modes). Boost pressure, spark timing and catalyst temperature are included in the discussion to explain the trends. Then, emissions are compared because of their strong dependence on some of the engine working parameters, which must be also considered to explain the effect of the fuel used. Regarding the accelerations, results presented in this section are the average of the 10 toothsaw accelerations. The error bars in the figures are defined as the confidence interval (95% confidence level).

3.1. Power Output and Acceleration

Maximizing power output and efficiency is the main goal of high-octane gasoline fuels, as detailed in the introduction. Figure 3 represents the acceleration and power output (power at the wheels) for the three gasolines tested during the toothsaw accelerations. Vehicle acceleration depends on the difference between the traction force in the wheels (which depends on the effective torque delivered by the engine) and the resistance forces, calculated through the coastdown test and imposed by the dyno. At each velocity, the traction force, and hence the vehicle acceleration, increases with the engine torque. The power delivered (Figure 3a) by the high-octane fuels (98 and 100 RON gasolines) is higher compared to 95 RON gasoline. This increase is not uniform throughout the whole velocity and octane ranges, but is sharper for the 100 RON fuel and when velocity is higher than 60–70 km/h (around 2500 rpm). This is consistent with the results of acceleration time (Figure 3b). As illustrated, the higher power delivered by the 100 RON gasoline produced the highest acceleration and thus the shortest time to reach the final velocity goal (162 km/h). 98 and 100 RON gasolines reduced the acceleration duration (compared to 95 RON) by 2.7% and 6.7%, respectively. During the steady-state modes, the power in the wheels (Figure 3) increased with the octane number of the fuels, and again the effect was more significant with the 100 RON gasoline. The 98 RON gasoline increased power by 3.4%, while this number increased up to 7.7% with the highest-octane gasoline (both compared to 95 RON gasoline).

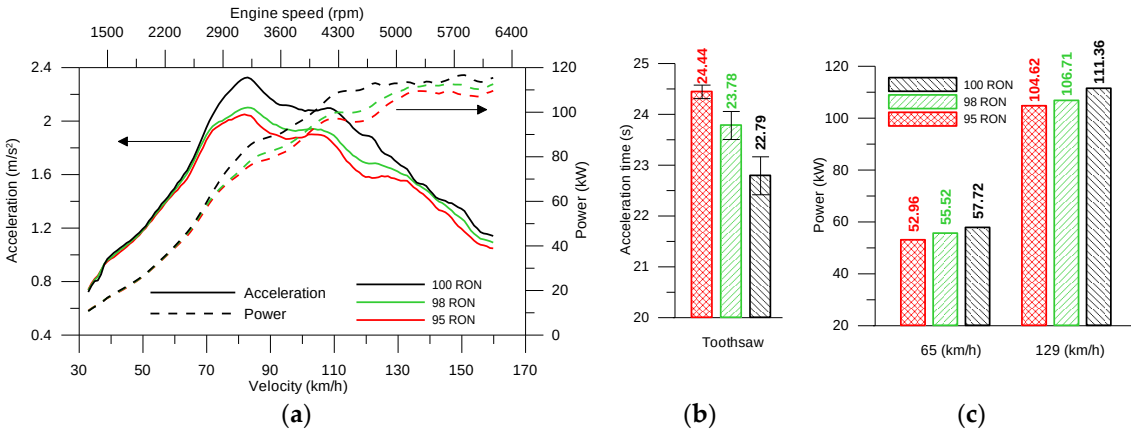

Figure 3. (**a**) Acceleration and power output along the toothsaw, (**b**) total acceleration time for toothsaw and (**c**) power output for steady-state modes.

As described in the introduction, current SI engines can adapt some operating parameters (boost pressure and spark timing advance, mainly) depending on the gasoline autoignition resistance in order to protect the engine against knocking and to reach the highest power output. Therefore, evaluating these parameters (and others that are affected by the operating parameters, such as the exhaust temperature) is necessary to explain the power and acceleration differences.

Turbocharging (increasing boost pressure) is one of the current tendencies in SI engines to improve the power output and efficiency. The intake air flow rate increases with the boost pressure; thus, more fuel can be admitted in the mixture, increasing the power. However, boost pressure is limited as it contributes to knocking due to the higher pressure and temperature at the beginning of the compression stroke. The tested vehicle incorporates a boost pressure control system (based on commanding a waste-gate valve in the turbine) managed by the ECU.

Figure 4 shows the boost pressure and the temperature upstream catalyst, which is directly related to the position of the waste-gate valve, for all the fuels and engine modes tested. Regarding the toothsaw accelerations (Figure 4a), boost pressure and air mass flow rate were higher for 100 RON gasoline, especially in the range between 70 to 130 km/h, with no significant differences between the other two fuels. This is because the higher knocking resistance of 100 RON gasoline allowed higher boosting without knocking. This velocity range (70–130 km/h) agrees well with the range where power and acceleration were the highest for the 100 RON fuel (Figure 3), which points to the boost pressure control system as the main factor contributing to the outstanding performance of this fuel.

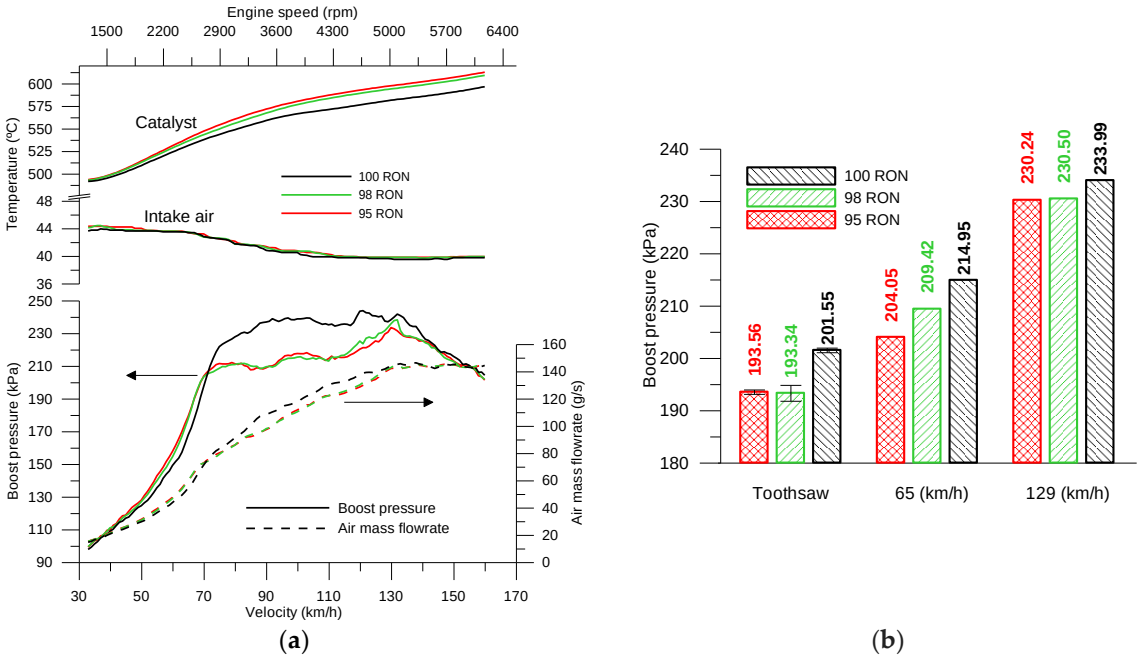

Figure 4. (**a**) absolute boost pressure, air mass flow rate, upstream catalyst temperature and intake air temperature along the toothsaw, (**b**) average absolute boost pressure along toothsaw and steady-state modes.

Boost pressure values were consistent with the exhaust temperature upstream of the three-way catalyst (Figure 4a). The higher boost pressure with the 100 RON gasoline is achieved by increasing the exhaust flow rate that passes through the turbine (i.e., decreasing the exhaust fraction that by-pass the turbine through the waste-gate valve). Since the gas temperature decreases in the turbine, as dictated by the gas dynamics in this device, the lower exhaust temperature with the 100 RON gasoline is a consequence of the lower waste-gate valve opening. As observed in Figure 4, the intake temperature was the same for all fuels and then could not contribute to the differences found in the exhaust gas temperature. Similar results were found at both steady-state modes (Figure 4b), with 100 RON gasoline having the highest boost pressure. In the 65 km/h mode, an increase in boost pressure with the 98 RON gasoline (compared to 95 RON) was observed as well, which indeed supports its higher power (Figure 3b).

Lambda sensor values are displayed in Figure 5 and reveal the calibration strategy of the engine; moreover, lambda values are decisive to explain the emissions. As it is typical in these sensors, there are two voltage levels (around 0.1 V and 0.9 V for lean and rich combustion, respectively) and a rapid, step-like transition zone around stoichiometric combustion. Along the toothsaw accelerations, the engine started running with oxygen excess (lean) at low engine speed (below 1500 rpm) for a short time. After pressing the gas pedal wide open, the throttle valve opens abruptly and there is a sudden increase in the air mass flow that lead to a brief lean operation. After that, the combustion moved to near-stoichiometric fuel-air ratio, and slightly richer as the speed increases up to 3300 rpm, approximately. From 3300 rpm onwards, the combustion became extremely rich. Consistently with the boost pressure trend, average lambda values scaled inversely with the octane number of the fuel (Figure 5b) indicating less rich combustion as the octane number is increased. This was demonstrated in the accelerations and in both steady-state modes.

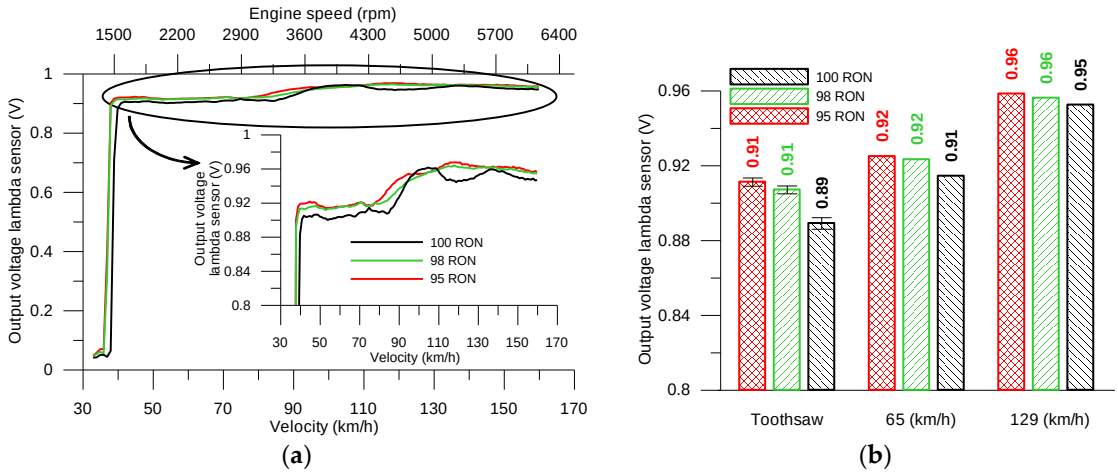

Figure 5. (**a**) Lambda values along the toothsaw, (**b**) average lambda values along toothsaw and steady-state modes.

Spark ignition advance is another parameter that affects the engine performance. As revised in the introduction section, there is an optimal ignition timing (MBT) that maximizes the output torque and the engine efficiency. SI engines do not usually work at MBT conditions, at least not in the whole speed and torque range, since this would lead to severe permanent knocking. Hence, spark timing advance is typically delayed with respect to MBT and this reduces the effective torque available. In the toothsaw accelerations (Figure 6a), two different trends were observed depending on the speed range. First, from the beginning to 70 km/h the spark ignition is more advanced as the octane number of the fuel is increased. Then, from 70 km/h onwards, the differences in the spark timing of the fuels are less significant, and the more advanced spark ignition remains only with the 98 RON gasoline. As observed, the cut point velocity of both ranges (70 km/h) coincides well with the velocity from which the boost pressure (Figure 4a) starts to be sensitive to the fuel. This could indicate that the internal control algorithms of both variables under transient accelerations are coupled in this engine. By contrast, when the steady-state modes were tested (Figure 6b), a slightly more advanced spark timing was measured with the increase of the octane number (around 1 °CA for the 100 RON gasoline, compared to 95 RON, with a linear trend between fuels).

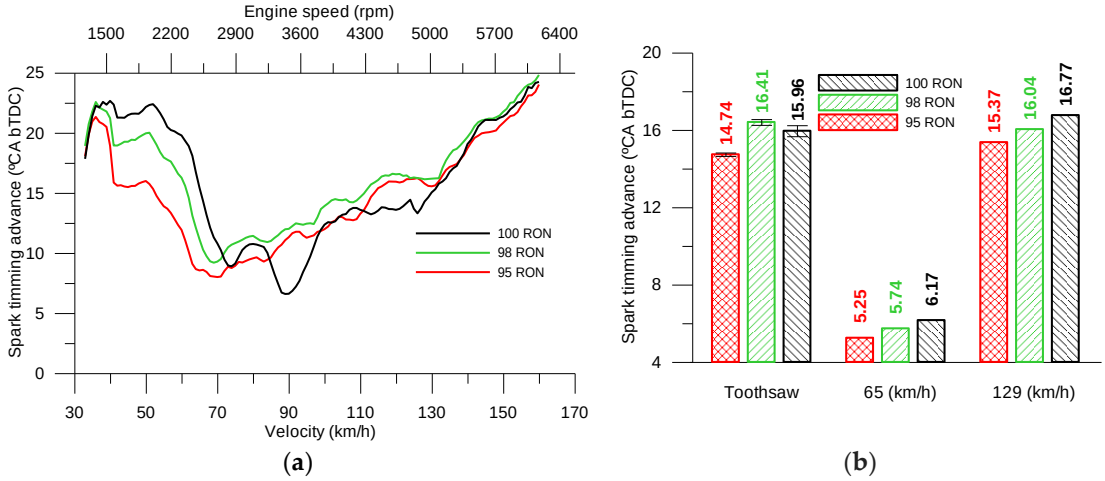

Figure 6. (**a**) Spark ignition advance along the toothsaw, (**b**) average spark ignition advance along toothsaw and steady-state modes.

3.2. Specific Fuel Consumption

The specific fuel consumption is shown in Figure 7. Fuel consumption is calculated based on a carbon balance method, as stated in the section devoted to the experimental setup. Since the three tested fuels have close heating values, the specific fuel consumption is inversely proportional to the engine efficiency. There is a marked decrease in the specific fuel consumption with the increase in octane number, this effect being more notable in the toothsaw accelerations. Compared to 95 RON gasoline, 98 and 100 RON gasolines decreased the specific fuel consumption in the toothsaw accelerations by 5% and 12%, respectively; these figures were reduced to 2.8% and 8.3% (average) in the steady-state modes. As observed, the fuel save of the 100 RON gasoline was superior than that of the 98 RON gasoline, even in relative terms. By contrast, other authors [5] reported a linear benefit of increasing RON on the fuel consumption when running driving cycles. This is because knocking is a phenomenon extremely dependent on the engine design, engine calibration and operating conditions. Although higher RON may be positive for a wide range of vehicles equipped with knock control devices, the exact magnitude and the proportionality of the benefits depends on the combination of these factors.

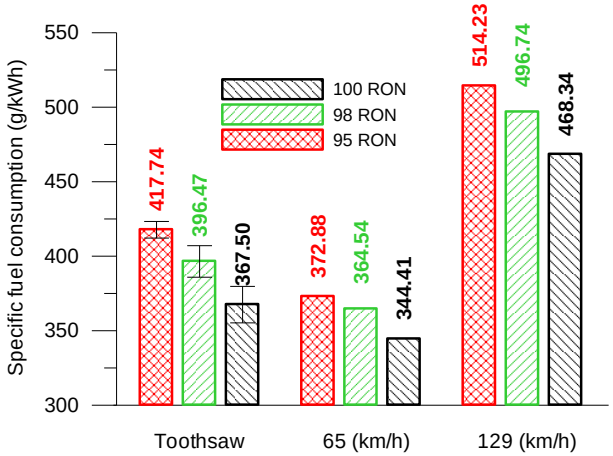

Figure 7. Average specific fuel consumption along toothsaw and steady-state modes.

The positive effect of the octane number on the fuel economy and the efficiency is a combination of two factors. First, under rich conditions (Figure 5), the higher intake air flow rate with high-octane fuels (Figure 4a), derived from the higher boost pressure, leads to more energy release from the fuel

which increases the indicated torque and consequently the mechanical efficiency. Second, the more advanced ignition (Figure 6) increases the thermal efficiency of the cycle.

3.3. Gaseous Emissions

During the whole cycle (toothsaw and steady-state modes), the gaseous emissions were measured continuously. Figure 8 shows CO_2, CO, THC and NOx emissions during the toothsaw acceleration. Several regions are observed in the figure. From the beginning to 55–60 km/h, there were no significant CO and THC emissions. This is a consequence of the initial lean operation (as indicated by the lambda sensor, Figure 5a) and the subsequent operation at near-stoichiometric conditions (optimal conditions for the three-way catalyst), where the CO and THC generated in the combustion chamber were abated in the three-way catalyst. In this first region, CO_2 emission increased slowly, proportionally to the power. Most of the total NOx in the accelerations were emitted in this region, where NOx reached a peak (see Figure 7b) because the catalyst could not reduce the engine-out NOx under the initial lean conditions. In the second region (from 55 km/h to around 90 km/h), both CO_2 and CO increased with the velocity, being this increase approximately linear and steeper in the case of CO_2. THC emissions also increased. These trends agree well with the lambda sensor values in this velocity range (55–90 km/h), which indicated a progressive and slow transition from near-stoichiometric to slightly rich combustion. There is a last region (from 90 km/h) where the CO_2 emission stabilized, while THC and CO continued to increase with the velocity. The rate of increase was higher than in the previous region (this is more evident in the CO trace, Figure 8a, which reached even higher values than CO_2) because more fuel is consumed to respond to the acceleration demand, but it is not oxidized completely to CO_2. Again, this is consistent with the lambda values, which indicated a faster shift towards much richer combustion. Even the final stabilization of the CO emission agrees with the stabilization of the lambda values.

For 100 RON gasoline, in the last velocity region there was a trade-off between CO_2 and CO/THC (when the former increased the others decreased, and vice versa), especially evidenced by fluctuations around a trend line in the emission flow rate profiles (Figure 8a). Under oxygen-limited conditions, fuel molecules compete for the available oxygen in the combustion chamber: when oxygen becomes more accessibility to fuel molecules (more homogeneous mixture, higher turbulence, etc.), CO_2 increases and CO/THC decrease. Also, the three-way catalyst plays a role in the final CO/CO_2 values, since in the absence of oxygen (rich combustion) a water gas shift reaction may occur [30]. These processes in the combustion chamber and the catalyst may be the cause for the aforementioned trends for CO and CO_2.

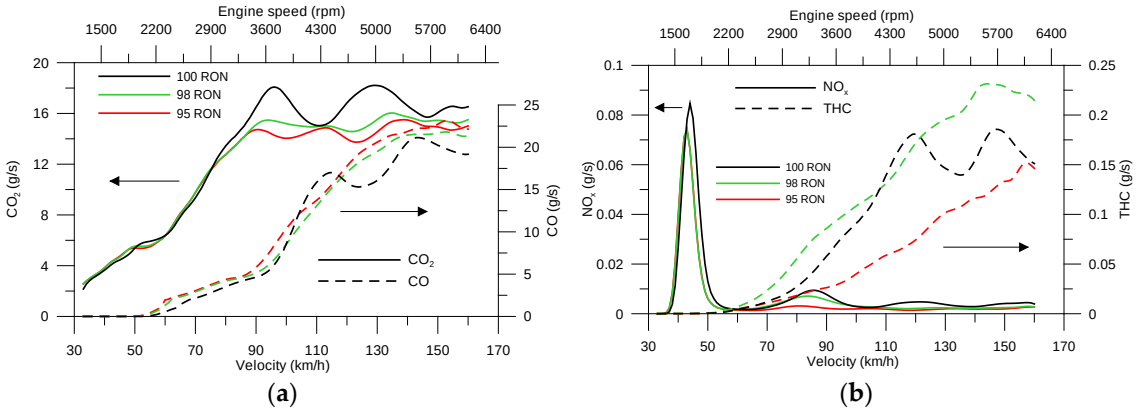

Figure 8. CO_2 and CO emissions (**a**) and NO_x and total hydrocarbon (THC) emissions (**b**) along toothsaw.

Regarding the effect of the fuel, the CO_2 flow rate increased with the octane number, whereas CO decreased (Figure 8a) at velocities higher than 70 km/h (approximately). The main responsible factors are the higher intake air flow rate in the case of 100 RON gasoline, compared to 95 RON (leading to lower fuel enrichment), and the more advanced ignited in the case of 98 RON gasoline, both

factors contributing towards a more complete combustion. When the specific CO_2 and CO emissions (g/kWh) are discussed (Figure 9a,b), CO_2 was not affected by the fuel because the octane number contributed to higher power and this counteracted the higher CO_2 flow rate, but CO was greatly reduced with increasing octane number. Compared to 95 RON gasoline, 98 and 100 RON gasolines decreased the specific CO emission by 9% and 20%, respectively, and the trend is consolidated in both the accelerations and the steady-state modes.

There was not a clear tendency of specific THC emissions (Figure 9d) with the octane number of the fuel, with the intermediate RON fuel showing the highest values in all the tests. Nevertheless, the fuel effect, if any, is probably masked by the very low concentration emitted compared to that of CO. Low THC and high CO emissions confirm that the oxygen available on the combustion chamber is enough to initiate the combustion reactions of the fuel hydrocarbons but not to complete them. Finally, NOx emissions were in general higher for higher octane fuels (except in the steady-state mode at 65 km/h, Figure 9c), probably on account of the higher combustion temperatures derived from the lower fuel enrichment and the higher intake temperature (due to the increased boost pressure).

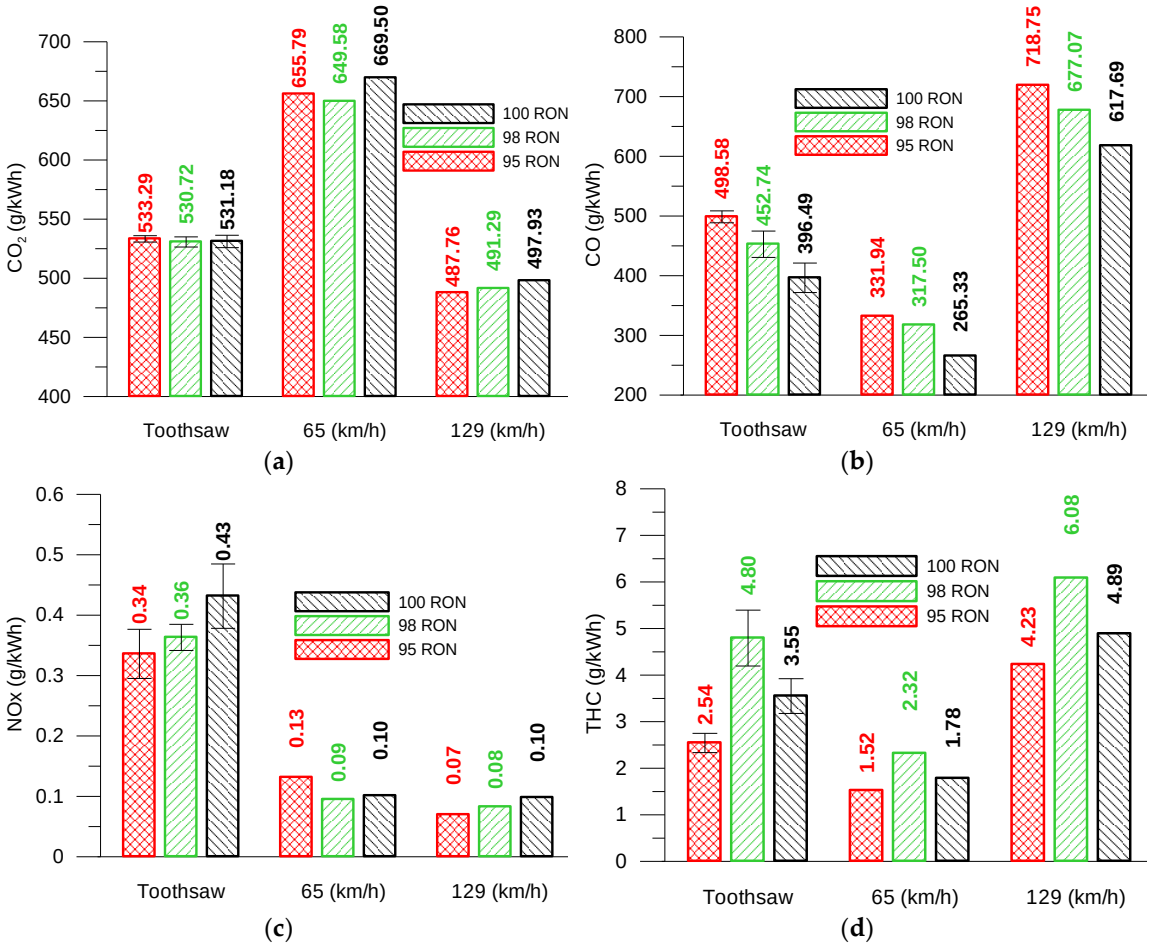

Figure 9. CO_2 (**a**), CO (**b**), NOx (**c**) and THC (**d**) emissions.

4. Conclusions

The potential of high-octane gasolines to increase fuel economy and thermal efficiency has been evaluated in a Euro 6b passenger car running at full load accelerations and two steady conditions. The results have proved that high octane number can be exploited by current and future SI engine technologies, with no penalization or some benefits in gaseous emissions.

High-octane fuels led to increased power and acceleration and reduced specific fuel consumption. The effect of the octane number was nonlinear, with 98 RON improving the base case (95 RON)

moderately, but 100 RON improving it greatly. As an example, 98 and 100 RON gasolines reduced the acceleration duration (compared to 95 RON) by 2.7% and 6.7%, respectively. Moreover, the power gain was not uniform in the whole speed range: at low velocity there was no significant effect whereas in the middle range the effect was highly marked. The main reasons supporting these results were the higher boost pressure (specially with 100 RON gasoline) and the advanced spark timing (specially with 98 RON). The electronic control unit of the engine manages both parameters conveniently to avoid knocking, which is detected through a knock sensor equipped in the vehicle.

Octane number did not affect THC or NOx emissions significantly, although the latter slightly increased with the 100 RON fuel. Regardless of the fuel, a NOx peak was manifested at the start of the accelerations because of a momentary lean operation. CO emission was reduced with the octane number, which was a consequence of the higher air-to-fuel ratio derived from the higher boost pressure.

Author Contributions: Conceptualization, D.C. and J.D.; Data curation, Á.R.; Formal analysis, J.R.-F. and Á.R.; Funding acquisition, J.D.; Investigation, Á.R. and J.B.; Methodology, J.R.-F., Á.R., J.B. and D.C.; Project administration, J.R.-F. and J.D.; Resources, J.D.; Software, Á.R.; Supervision, D.C. and J.D.; Validation, Á.R.; Visualization, D.C. and J.D.; Writing—original draft, J.R.-F., Á.R. and J.B.; Writing—review & editing, J.R.-F., Á.R., J.B., D.C. and J.D. All authors have read and agreed to the published version of the manuscript.

Funding: This activity is included on the Project "Desarrollo de gasolina para motores eficientes" that has been partially funded by Spanish CDTI (Centro de Desarrollo Tecnológico Industrial), identified as IDI-20180217.

Conflicts of Interest: The authors declare no conflict of interest.

References

1. European Commission. A European Green Deal: Striving to be the First Climate-Neutral Continent. 2019. Available online: https://ec.europa.eu/info/strategy/priorities-2019-2024/european-green-deal_en (accessed on 6 July 2020).
2. European Environment Agency. Greenhouse Gas Emissions from Transport in Europe. 2019. Available online: https://www.eea.europa.eu/data-and-maps/indicators/transport-emissions-of-greenhouse-gases/transport-emissions-of-greenhouse-gases-12 (accessed on 6 July 2020).
3. Knuutila, L. Blending Strategies and Process Modification for the Future Gasoline Production. Master's Thesis, Programme in Advance Energy Solutions. Aalto University, Espoo, Finland, 2019.
4. Kalghatgi, G. Developments in internal combustion engines and implications for combustion science and future transport fuels. *Proc. Combust. Inst.* **2015**, *35*, 101–115. [CrossRef]
5. Williams, J.; Hamje, H. *Testing and Modelling the Effect of High Octane Petrols on an Adapted Vehicle*; Technical Report No. 8/20; Concawe: Brussels, Belgium, 2020. Available online: https://www.concawe.eu/wp-content/uploads/Rpt_20-8.pdf (accessed on 6 July 2020).
6. Stradling, R.; Williams, J.; Hamje, H.; Rickeard, D. Effect of Octane on Performance, Energy Consumption and Emissions of Two Euro 4 Passenger Cars. *Transp. Res. Procedia* **2016**, *14*, 3159–3168. [CrossRef]
7. Kalghatgi, G. Knock onset, knock intensity, superknock and preignition in spark ignition engines. *Int. J. Engine Res.* **2017**, *19*, 7–20. [CrossRef]
8. Pan, J.; Shu, G.; Wei, H. Interaction of Flame Propagation and Pressure Waves during Knocking Combustion in Spark-Ignition Engines. *Combust. Sci. Technol.* **2014**, *186*, 192–209. [CrossRef]
9. Kalghatgi, G.T.; Bradley, D. Pre-ignition and 'super-knock' in turbo-charged spark-ignition engines. *Int. J. Engine Res.* **2012**, *13*, 399–414. [CrossRef]
10. Hamilton, L.J.; Rostedt, M.G.; Caton, P.A.; Cowart, J.S. Pre-Ignition Characteristics of Ethanol and E85 in a Spark Ignition Engine. *SAE Int. J. Fuels Lubr.* **2008**, *1*, 145–154. [CrossRef]
11. Dahnz, C.; Han, K.-M.; Spicher, U.; Magar, M.; Schiessl, R.; Maas, U. Investigations on Pre-Ignition in Highly Supercharged SI Engines. *SAE Int. J. Engines* **2010**, *3*, 214–224. [CrossRef]
12. Manz, P.W.; Daniel, M.; Jippa, K.N. Pre-ignition in highly charged turbo-charged engines. Analysis procedure and results. In Proceedings of the 8th International Symposium on Internal Combustion Diagnostics, Baden-Baden, Germany, 10–11 June 2008.
13. Wang, Z.; Liu, H.; Song, T.; Qi, Y.; He, X.; Shuai, S.; Wang, J. Relationship between super-knock and pre-ignition. *Int. J. Engine Res.* **2014**, *16*, 166–180. [CrossRef]

14. Ceschini, L.; Morri, A.; Balducci, E.; Cavina, N.; Rojo, N.; Calogero, L.; Poggio, L. Experimental observations of engine piston damage induced by knocking combustion. *Mater. Des.* **2017**, *114*, 312–325. [CrossRef]
15. Bi, F.; Ma, T.; Wang, X. Development of a novel knock characteristic detection method for gasoline engines based on wavelet-denoising and EMD decomposition. *Mech. Syst. Signal Process.* **2019**, *117*, 517–536. [CrossRef]
16. Feng, D.; Buresheid, K.; Zhao, H.; Wei, H.; Chen, C. Investigation of lubricant induced pre-ignition and knocking combustion in an optical spark ignition engine. *Proc. Combust. Inst.* **2019**, *37*, 4901–4910. [CrossRef]
17. Shao, J.; Rutland, C.J. Modeling Investigation of Different Methods to Suppress Engine Knock on a Small Spark Ignition Engine. *J. Eng. Gas Turbines Power* **2015**, *137*, 061506. [CrossRef]
18. Lim, G.; Lee, S.; Park, C.; Choi, Y.; Kim, C. Effect of ignition timing retard strategy on NOx reduction in hydrogen-compressed natural gas blend engine with increased compression ratio. *Int. J. Hydrogen Energy* **2014**, *39*, 2399–2408. [CrossRef]
19. Szybist, J.; Foster, M.; Moore, W.R.; Confer, K.; Youngquist, A.; Wagner, R.M. Investigation of Knock Limited Compression Ratio of Ethanol Gasoline Blends. *SAE Paper* **2010**. [CrossRef]
20. Grandin, B.; Denbratt, I.; Bood, J.; Brackmann, C.; Bengtsson, P.-E.; Gogan, A.; Mauss, F.; Sundén, B. Heat Release in the End-Gas Prior to Knock in Lean, Rich and Stoichiometric Mixtures with and without EGR. *SAE Paper* **2002**. [CrossRef]
21. Wei, H.; Zhu, T.; Shu, G.; Tan, L.; Wang, Y. Gasoline engine exhaust gas recirculation—A review. *Appl. Energy* **2012**, *99*, 534–544. [CrossRef]
22. Grandin, B.; Ångström, H.-E. Replacing Fuel Enrichment in a Turbo Charged SI Engine: Lean Burn or Cooled EGR. *SAE Paper* **1999**. [CrossRef]
23. Wang, Z.; Liu, H.; Reitz, R.D. Knocking combustion in spark-ignition engines. *Prog. Energy Combust. Sci.* **2017**, *61*, 78–112. [CrossRef]
24. Zhen, X.; Wang, Y.; Xu, S.; Zhu, Y.; Tao, C.; Xu, T.; Song, M. The engine knock analysis—An overview. *Appl. Energy* **2012**, *92*, 628–636. [CrossRef]
25. Li, T.; Yin, T.; Wang, B.; Qiao, X. Determination of Knock Limited Spark Advance in Engine Cycle Simulation. In Proceedings of the International Symposium on Diagnostics and Modeling of Combustion in Internal Combustion Engines, Okayama, Japan, 25–28 July 2017; Japan Society of Mechanical Engineers: Tokyo, Japan, 2017; p. A103.
26. Shen, Y.T.; Wang, J.Z.; Shuai, S.J.; Wang, J.X. Effects of octane number on gasoline engine performance. *Chin. Int. Combust. Engine Eng.* **2008**, *29*, 52–56.
27. Shuai, S.-J.; Wang, Y.; Li, X.; Fu, H.; Xiao, J. Impact of Octane Number on Fuel Efficiency of Modern Vehicles. *SAE Int. J. Fuels Lubr.* **2013**, *6*, 702–712. [CrossRef]
28. European Automobile Manufacturers Association (ACEA); European Medicines Agency; JAMA. *Worldwide Fuel Charter: Gasoline and Diesel Fuel*, 6th ed. 2019. Available online: https://www.acea.be/uploads/publications/WWFC_19_gasoline_diesel.pdf (accessed on 6 July 2020).
29. European Commission. Regulation 2017/1151 of 1 June 2017 supplementing Regulation (EC) No 715/2007 (. . .) to emissions from light passenger and commercial vehicles (Euro 5 and Euro 6) (. . .). *Off. J. Eur. Union* 02017R1151, 1-839. **2017**.
30. Han, Z.; Wang, J.; Yan, H.; Shen, M.; Wang, J.; Wang, W.; Yang, M. Performance of dynamic oxygen storage capacity, water–gas shift and steam reforming reactions over Pd-only three-way catalysts. *Catal. Today* **2010**, *158*, 481–489. [CrossRef]